Study and Suppression of Multipath Signals in a Non-Invasive Millimeter Wave Transmission Glucose Sensing System

Maria Koutsoupidou, Helena Cano-Garcia, Roberto L. Pricci, Shimul C. Saha, George Palikaras, Efthymios Kallos and Panagiotis Kosmas, *Senior Member, IEEE*

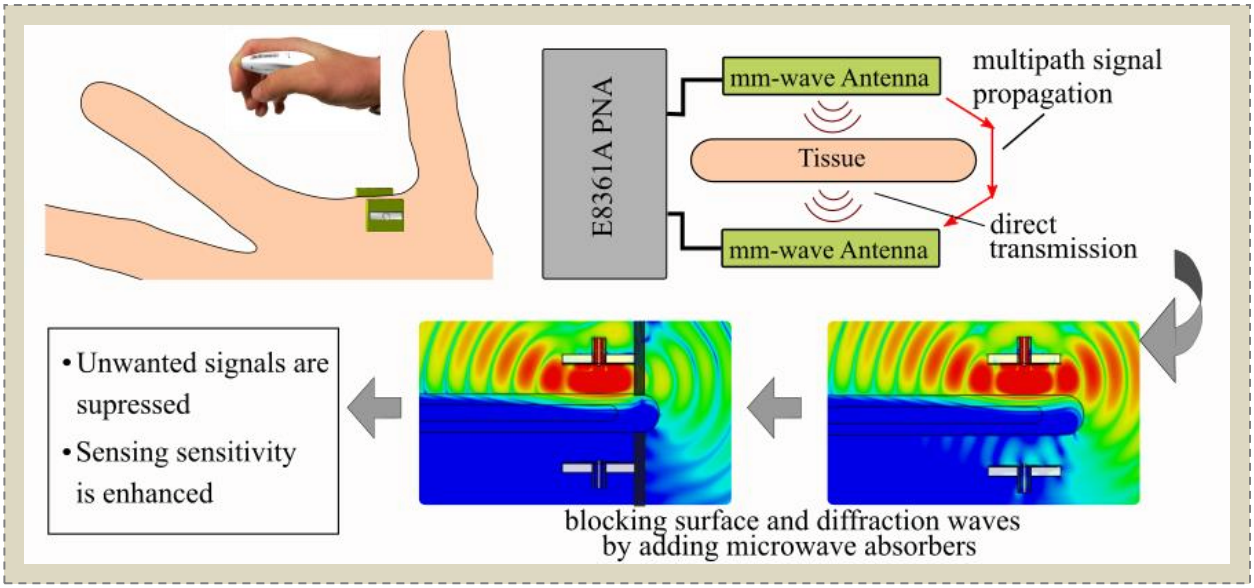

Multipath signals can dominate millimeter (mm)-wave transmission measurements and must be suppressed for non-invasive mm-wave glucose sensing.

- The paper studies the significant impact of multipath wave propagation (surface and diffraction waves) on electromagnetic (EM) sensing systems, which is often overlooked in the design and development of EM sensors.
- System simulations and experimental results with a millimeter (mm)-wave sensor demonstrate the need to suppress these unwanted signals in order to increase EM sensing sensitivity.
- Experimental measurements demonstrate that sensor's sensitivity to glucose concentrations is almost doubled by suppressing multipath waves with appropriate use of absorbers.
- Our study focuses on sensing glucose changes with mm-waves, but this analysis can be useful for any application in EM biomedical sensing which requires the detection of weak signals propagating through lossy tissues.

Study and Suppression of Multipath Signals in a Non-Invasive Millimeter Wave Transmission Glucose Sensing System

Maria Koutsoupidou, Helena Cano-Garcia, Roberto L. Pricci, Shimul C. Saha, George Palikaras, Efthymios Kallos and Panagiotis Kosmas, *Senior Member, IEEE*

Abstract Electromagnetic (EM) biomedical sensors in the mm-wave frequency range must detect small changes in signals in the presence of tissues, which are correlated to a pathological condition. These signals, however, can suffer from artifacts due to complex EM wave interactions such as diffraction and surface wave propagation, which are often overlooked in the design phase of these sensors. This paper studies the impact of these wave phenomena on the signals transmitted and received from a pair of antennas designed to sense glucose changes via changes in transmission through a sample. Numerical simulations and controlled experiments with glucose solutions demonstrate for the first time that unwanted signal contributions from mm surface waves along the tissue can dominate the received signals but can be reduced with the use of appropriately placed absorbers around the antenna sensors. As a result, the sensitivity of such a sensing system to glucose changes is increased. This finding can be very useful in the design and development of the glucose sensor under study, as well as for other EM-based diagnostic medical applications.

***Keywords* — chemical and biological sensors, electromagnetic propagation, electromagnetic modeling, millimeter wave measurements, surface waves**

I. Introduction

ELECTROMAGNETIC (EM) waves are promising for certain challenging diagnostic medical applications such as non-invasive glucose monitoring [1]. Various glucose sensing systems have been developed based on EM waves in the microwave [2], [3], infrared (IR) [4], [5] and optical frequency range [4], [6]. Amongst these different wavelengths, mm-waves are suitable for glucose sensing as their penetration depths allow sub-skin interaction with human tissue. Moreover, mm-wavelengths are short enough to enable the development of compact sensors.

Based on these considerations, a non-invasive biomedical system for blood glucose sensing is currently under development by MediWise Ltd, which combines mm-waves with transmission-based sensing [7], [8]. Water absorption is maximized in the mm-wave range for normal body temperatures [9]. Therefore, the mm-wave signals transmitted and processed by the system will experience significant attenuation as they propagate through lossy water-based tissue [10]. This effect causes large changes in the dielectric properties and hence the transmission for varying glucose levels [1]. Detecting small changes requires a sensitive receiver capable of detecting very weak signals (<-50 dB), and the ability to extract diagnostic information from small changes in the total received signals.

Beyond glucose sensing, various biomedical imaging and sensing applications process information acquired from EM wave transmission through tissues [11], [12]. In these systems, diagnostically useful data are extracted from spatial and/or temporal changes in the dielectric properties of the tissue, as these changes impact the EM signals transmitted through the interrogated region. Total received signals include components from line-of-sight transmission, diffraction, and surface wave propagation. Multipath signals can obscure the useful response from the total received signals, and are thus usually undesired [13], [14].

Tackling this problem with hardware depends on the type of application and system design. In microwave tomography, for example, the system is immersed in a high-loss liquid which can suppress unwanted multipath propagation [15], [16]. However, this causes additional attenuation in the diagnostically useful transmitted signals, which would be prohibitive in shorter-wavelength mm-wave applications such as glucose sensing. It is therefore critical to understand the behavior of such multipath signals and find methods to suppress them.

The concept of using absorbers to suppress multipath signals is likely to be considered in practical systems or experiments processing microwave signals. To the best of our knowledge, however, this paper presents a unique study which for the first time quantifies the effects of multipath

Manuscript received on April 05, 2019;
This work was supported in part by Innovate UK grant number 103862.

M. Koutsoupidou, H. Cano-Garcia and P. Kosmas are with the Department of Informatics, King's College London, London, Strand Campus, UK (correspondence e-mail: maria.koutsoupidou@kcl.ac.uk).

H. Cano-Garcia, S. C. Saha, R. L. Pricci, G. Palikaras, E. Kallos and P. Kosmas are with MediWise, Medical Wireless Sensing Ltd., London, UK and Metamaterial Technologies Inc., Dartmouth, NS B2Y 4M9, Canada. (correspondence e-mail: themos.kallos@metamaterial.com).

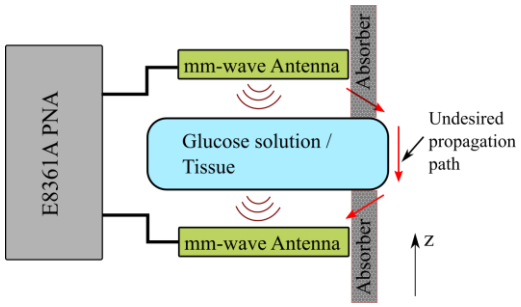

Figure 1. Block diagram of the system setup. A pair of sensors interacts with the sample/tissue. Transmission measurements are recorded using a network analyzer. The red arrows indicated the prime undesirable propagation path that affects the main signal.

signals and benefits of using absorbers for a practical transmission-based sensing system in the vicinity of biological tissues, by means of both accurate numerical simulations and experimental measurements. Moreover, by illustrating the need to place absorbers for the proposed compact sensor, the paper leads to a novel design for our glucose system, which has not appeared in the literature previously. The study proposes to enhance the sensitivity (change in transmission S_{21} for a given glucose level change) of MediWise's current mm-wave glucose sensing system, by using absorbers to minimize unwanted signal propagation around the interrogated tissue. This is first illustrated in full-wave EM simulations with a skin tissue model. Then, simulations and measurements of transmission through glucose solutions of different concentrations with and without the absorbers demonstrate that the system's sensitivity to glucose changes is almost doubled by blocking these waves from reaching the receiving antenna.

II. Materials and Methods

A. System Setup

The experimental setup for non-invasive glucose measurements comprises two mm-wave antennas operating at 37 GHz connected to a Vector Network Analyzer (VNA) (Fig. 1). This frequency range was selected as it can provide adequate penetration into the tissue and resolution, and readily available electronics [7]. The antenna sensors are mounted on a custom-made 3D printed support for placing a human hand. The setup also allows placements of phantoms or containers filled with glucose solutions for testing the system. Two stepper motors allow optimizing the antennas' positions along the z-axis. Stable cables (Maury, Stability™) are used to minimize amplitude and phase drifts during measurements.

The employed antennas are modifications of a previous 60 GHz design [16], which has been scaled and optimized. They are based on a 12x14 mm^2 patch with a substrate thickness of 254 μm, dielectric constant (ε_r) of 2.2, and loss tangent (tanδ) of 0.0009 (RT/duroid® 5880 Laminate by Rogers Corporation).

To study the impact of multipath signals and the efficacy of placing absorbers to suppress them, the setup of Fig. 1 is tested in two different scenarios: a) a tissue numerical model consisting of skin and blood and b) a thin acrylic tank filled with water and a 5% glucose solution.

In the first scenario, the curved edges of the tissue cause emanating waves from the transmitting antenna to travel along the tissue surface and reach the receiving antenna. These surface waves can dominate the received signal, and their level depends on the multipath distance and the dielectric properties of the two mediums, i.e. skin and air. This process resembles surface wave propagation along planar or curved surfaces, which has been extensively studied [17].

In the second case of a thin tank filled with different glucose solutions, surface wave propagation is limited because there is no plane or curved surface connecting the two antennas. Diffraction by the tank's edges produces a more significant signal. This multipath phenomenon is less relevant to a practical measurement with our glucose sensor. However, the setup allows assessing the efficacy of the absorbers in blocking undesired signals in controlled experiments with varying glucose concentration solutions.

B. Microwave Absorber

For mm-wave glucose sensing, the measured tissue is thin and small, with thickness of a few mm. Thus, the antennas would be placed close to the edges of the tissue for sensor positions such as the earlobe or the thin skin area between the thumb and the index finger. Consequently, the absorbing material should be placed close to the antennas. At lower frequencies (not considered in this work), the examined tissue can be larger, but because of the longer wavelength and possibly the higher number of antennas [11], the absorbing material will always lie in the near field of the antennas.

To test the efficacy of EM absorbers for suppressing multipath transmission, two small rectangular slabs of the absorbing material are placed next to the antennas in the setup of Fig. 1. An effective absorber is usually made of a thin, non-conductive material with high EM attenuation at mm-wave frequencies. In this study, the Eccosorb GDS Microwave Absorber (Laird™, Missouri, USA) was chosen, which is a magnetically loaded silicone rubber sheet with a specification of almost 150 dB/cm attenuation at 40 GHz [18].

III. Numerical Simulations

A. Skin-Blood Tissue Simulations

A tissue model for the skin area between the thumb and the index finger was developed in CST Microwave Studio. The model mimics the curvature of the tissue and comprises three layers with a combined thickness of 7 mm: skin (2 mm) - blood (3 mm) - skin (2 mm). The dielectric properties of skin and blood at 40 GHz were set as ε_{skin} = 11.69, $\tan\delta_{skin}$ = 1.22, ε_{blood} = 17.53, $\tan\delta_{blood}$ = 1.18 [19]. The mm-wave antennas were placed symmetrically at

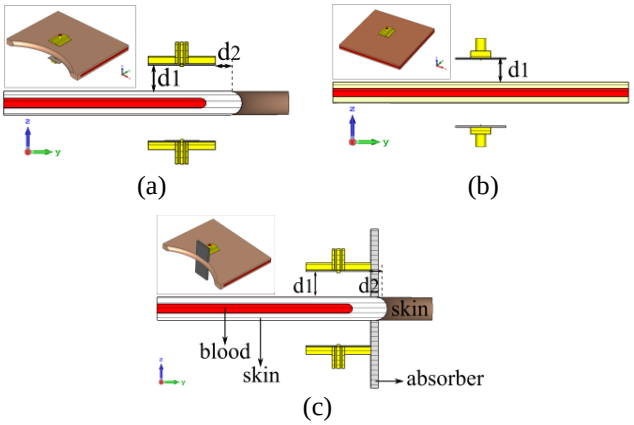

Figure 2. Simulation setups to study the impact of diffraction and surface waves with and without absorbers for two mm-wave antennas at distances d_1 = 5.5 mm from the skin surface and d_2 = 1.0 mm from the edge of the tissue: (a) curved skin and blood tissue model, (b) reference planar model of 80 mm x 80 mm size, and (c) curved tissue model with the absorbers.

distance d_1 = 5.5 mm from the tissue surface and distance d_2 = 1.0 mm from the edge of the tissue (Fig. 2(a)). The tissue lies in the antennas' near-field zone, and the distance d_1 minimizes the antenna's reflection coefficient, S_{11}: parametric analysis in the 35-40 GHz frequency range has shown that reflection coefficient is optimized for d1 = 5.5 mm with a resonance at 37 GHz.

To estimate the strength of signals due to multipath wave propagation, a reference model was simulated. The same setup was modelled, but the curved skin-blood tissue was replaced with one without curved edges (Fig. 2(b)). A third setup with the absorbing material was also modelled: a rectangular slab (15.2 mm x 16.5 mm x 1.6 mm) of the Eccosorb GDS material was added in front of each antenna (Fig. 2(c)). The slab's dimensions were selected to completely cover the antenna's side towards the edge of the skin tissue and the gap between the antenna and skin. The absorber is placed in contact with the antenna as the system must be as compact as possible in practice. The thickness of the absorbing material matches the commercially available choice. The dielectric properties of the GDS material are available in CST Microwave Studio. The 3rd order dielectric dispersion model provided in CST yields ε_{GDS} = 13.51 + i0.45 at 37 GHz. Open boundaries were set at the non-curved vertical surfaces of the tissue model for all simulation setups.

The electric field distribution on the yz plane of the setup without the absorbing material (Fig. 3(a)) clearly illustrates the propagation of strong signals along the curved skin surface at 37 GHz. The calculated transmission (S_{21}) and reflection coefficients (S_{11}) in the 35-40 GHz are shown in Fig. 3(c). For the reference setup, the signal transmitted through the skin and blood tissue has been attenuated by 110 dB at 37 GHz. However, when the curved tissue is used, the received signal at 37 GHz is -70 dB. The difference of 40 dB for the two setups suggests that, in actual measurements with distances similar to Fig. 2(a), waves propagating around and on the air-tissue interface significantly affect the received signal.

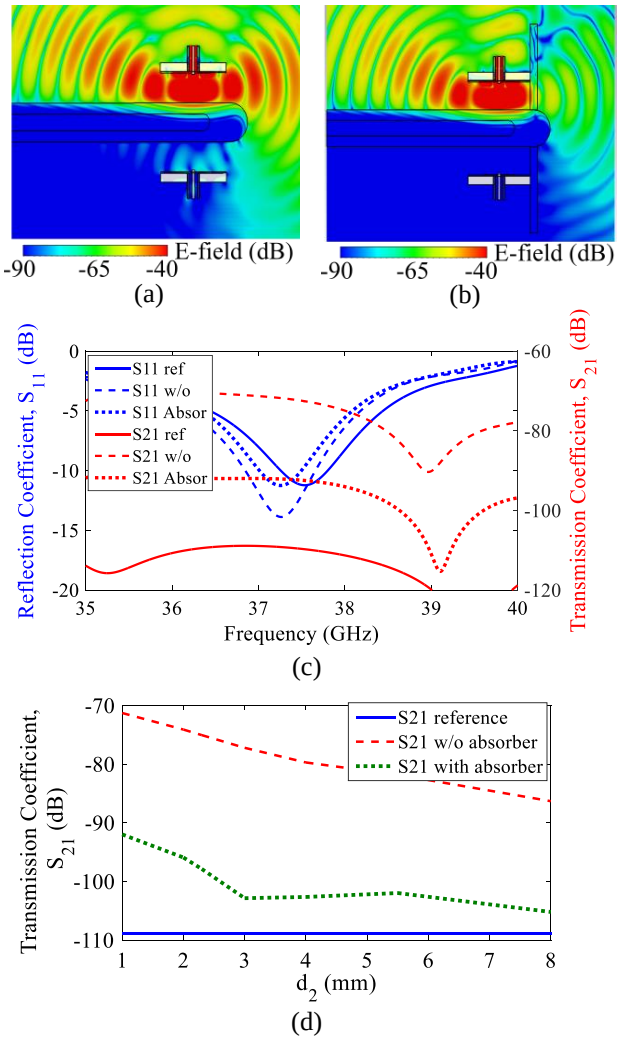

Figure 3. (a), (b) Electric field distribution on the yz plane of the skin and blood tissue model at 37 GHz: (a) without, and (b) with the absorbers. (c) Calculated reflection (S_{11}) and transmission (S_{21}) coefficients for the reference setup (solid line), the curved skin-blood tissue model (dashed line) and the curved skin-blood tissue model with absorbers (dotted line) in the 35-40 GHz range. (d) Calculated transmission (S_{21}) coefficients for the reference setup (solid line), without (dashed line) and with absorbers (dotted line) for different values of the distance d_2 at 37 GHz with the blood-skin model.

This difference will naturally depend on the thickness of the tissue. Evidently, the effect of these waves will decrease as the antennas are placed further from the edge of the tissue, as the total multipath propagation length will increase. This is illustrated by Fig. 3(d), which plots calculated transmission coefficients for different values of distance d_2. As the distance d_2 increases from 1 mm to 8 mm, S_{21} drops from -70 dB to -85 dB. This is still, however, 25 dB higher than the direct S_{21}, suggesting that the useful signals that travel through the tissue are "buried'' within the signals due to wave diffraction and surface propagation.

The absorbing material, on the other hand, significantly supresses these unwanted signal contributions. This is clearly visible qualitatively from comparing the E-field distributions in Figs. 3(a) and 3(b), and quantitatively by comparing the resulting S_{21} (dotted line) to the case without absorber (dashed line) in Figs. 2(c) and (d). For d_2 = 1 mm,

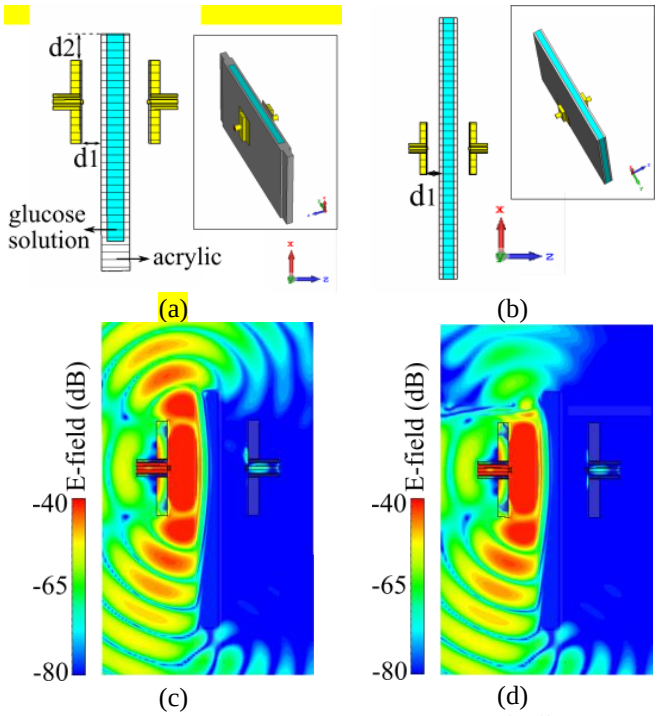

Figure 4. (a), (b) Simulation setup to study the impact of diffraction and surface waves with and without absorbers for controlled glucose experiments with a 1-3-1 tank model: (a)1-3-1 tank without the absorber and (b) reference setup. The mm-wave antennas are at a distance d_1 = 3.25 mm from the acrylic surface and d_2 = 4.0 mm form the upper edge of the tank. The absorbers will be added above the antennas. (c), (d) Electric field distribution on the yz plane at 37.7 GHz when the 1-3-1 tank is filled with DI water (gl 0 wt%): (b) without and (c) with the absorbers.

the interference signal is supressed and hence the transmission level drops to around -90 dB. In the case when the antennas are placed at d_2 = 3 mm from the edge of the skin, transmission also drops, this time to -105 dB. Importantly, the absorbing material does not affect the reflection coefficient S_{11} of the antenna plotted in Fig. 3(c), which shows an almost identical resonance at 37.2 GHz in both cases.

B. Simulations of Experiments with Glucose Solutions

To test our approach's efficacy in suppressing multipath signals and hence enhancing mm-wave glucose sensing, we simulated a controlled experiment with a setup comprising a thin tank filled with a solutions of varying glucose in de-ionised (DI) water [1]. The acrylic container has a volume capacity of 60x35x3mm^3 and 1-mm thick walls ("1-3-1 tank"). As shown in Fig. 4(a), the antennas were placed close to the top of the tank at a distance d_2 = 4.0 mm from the upper edge. Parametric analysis in the 35-40 GHz range has shown that optimal reflection coefficient S_{11} is achieved for antenna distance from the tank surface d_1 = 3.25 mm. The tank was initially filled with DI water ("gl 0 wt% concentration") and the simulations were repeated with a DI water/glucose solution ("gl 5 wt%"). The dielectric properties of these solutions were incorporated using two distinct Debye models, as in [1].

Similar to the analysis of Section III.A, two more setups were simulated. First, we modelled a reference setup as in

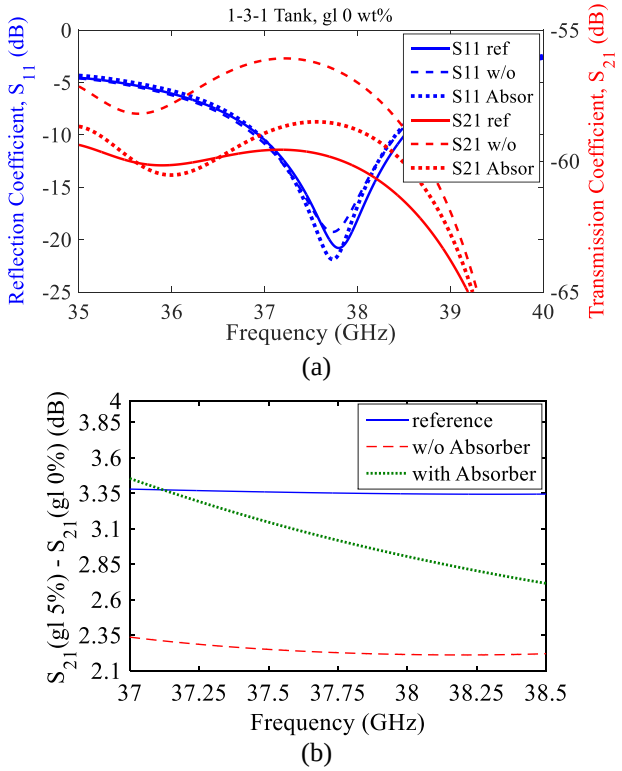

Figure 5. (a) Calculated reflection (S_{11}) and transmission (S_{21}) coefficients for the reference setup (solid line), the 1-3-1 tank model (dashed line) and the 1-3-1 tank model with absorbers (dotted line) in the 35-40 GHz range. (b) Calculated change (ΔS_{21}) in the measured transmission coefficient (S_{21}) due to the addition of 5 wt% glucose in DI water for the reference setup (solid line), the 1-3-1 tank with (dotted line) and without (dashed line) the absorbers.

Fig. 4(b) to evaluate direct transmission signal levels without multipath wave contributions. The antennas were placed across an 80 mm x 80 mm slab comprising three layers, acrylic (1 mm), liquid solution (3 mm), and acrylic (1 mm). Open boundaries were set at the non-vertical surfaces of the slab. Second, we modelled a setup similar to Fig. 4(a), but with added absorbers (Eccosorb GDS 15.2x16.5x1.6 mm^3 slabs), as in the case of the tissue simulations.

Electric field distributions with and without the GDS absorbing material on the xz plane of the 1-3-1 tank setup shown in Fig. 4(c), (d) confirm that the E-field is diffracted at the edges of the tank filled with the glucose solution. The fields were calculated at 37.7 GHz, where the antennas present a strong resonance in this simulation setup (see Fig. 5(a)). Comparison of the distributions in Fig. 4(c) and (d) shows clearly that placing an absorbing material perpendicular and close to the acrylic tank blocks a significant portion of this diffracted wave.

Figure 5(a) shows the transmission (S_{21}) and reflection (S_{11}) coefficients between 35-40 GHz for the three examined setups when the tank is filled with DI water only. As acrylic-water materials are less lossy than skin or blood and the total thickness of the tank is smaller than that of skin tissue, transmitted power levels for the tank setup are significantly higher than that of the skin tissue setup.

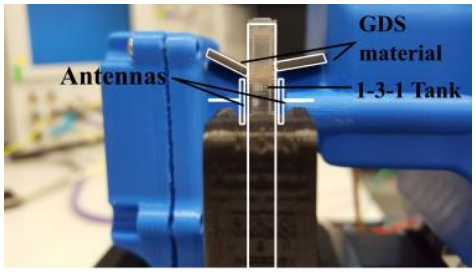

Figure 6. Experimental setup of the 3D printed base with two slabs of the Eccosorb GDS material on top of each antenna and the 1-3-1 tank placed between them.

Moreover, the impact of the signal generated by diffraction at the edges of the tank is less significant than surface wave propagation in Section III-A. Nevertheless, the transmitted signal at 37.7 GHz is still approximately 4 dB higher without an absorber than the 'reference' direct transmission, while it is only 1.5 dB higher with the absorber. This confirms the positive impact of the absorber for this simulation setup.

The placement of the absorbers also has a positive effect on the glucose sensing sensitivity of the system. To illustrate that, the simulations were repeated after replacing DI water with a DI water/glucose solution of gl 5 wt% concentration. The transmission response to the addition of glucose in DI water was calculated as difference in the S_{21} transmission, $\Delta S_{21} = S_{21}$(gl 5 wt%) $-S_{21}$(gl 0 wt%). The transmission difference ΔS_{21} was calculated with and without the absorber in the antennas' operating bandwidth 37.0 – 38.5 GHz and is plotted in Fig. 5(b). For the ideal reference case, this difference is ΔS_{21}=3.35 dB, and it is reduced to approximately 2.35 dB for the tank of finite dimensions in Fig. 4(a). With the use of the absorber, however, the transmission change increases by 0.5-1.0 dB, which is significant for these low signal levels.

IV. Experimental Results with Glucose Solutions

To confirm the previous findings with measurements, we used the same acrylic 1-3-1 tank as well as a 1-1-1 tank in experiments with DI water (gl 0 wt%) and a gl 5 wt% glucose solution. The tanks were placed between the antennas to perform sensitivity measurements with and without the absorbing material. The 1-1-1 tank contains 1/3 of the investigated liquid of the 1-3-1 tank and is useful to compare experimentally the absorbers' effect on signals experiencing different loss through transmission. A photo of the experimental setup is shown in Fig. 6.

Initially, each tank was filled with DI water (gl 0 wt%), and the antenna distance was adjusted using the stepper motors to achieve maximum transmission within the resonance spectrum of the antennas. The optimization process was performed only once, at the beginning of the experiment with DI water and without the absorbing material. The experimental protocol followed the steps below:

(1) Fill the tank with de-ionized water (gl 0 wt%);
(2) Measure and record;
(3) Remove the de-ionized water using a needle, and clean the tank using thin paper towel and left to dry;
(4) Fill the tank with the gl 5 wt% glucose solution;
(5) Measure and record;
(6) Remove the solution and wash the tank using fresh DI water, clean and left to dry;
(7) Repeat steps from (1) to (6) four more times.
(8) Repeat steps from (1) to (7) for a setup with two slabs of the Eccosorb GDS absorbing material placed above each antenna, as in Fig. 6

Keysight's E8361A PNA was used for the measurements with the following settings: averaging over 10 measurements, power -7 dBm, IF bandwidth of 10 Hz and 101 points spanning from 35 GHz to 39 GHz. The room temperature during the experiments was at 21 ± 0.2 ºC.

The measured transmission and reflection coefficients S_{21} and S_{11} (or S_{22}) with and without the absorbers are plotted in Figs. 7(a) and (b) for the two tanks filled with DI water (gl 0 wt%). Differences in the measured reflection coefficients S_{11}, S_{22} for the two antennas can be attributed to the non-symmetrical experimental setup and the fact that their distances from the tank are not equal, as they were positioned independently to optimize S_{11}. More importantly, the measured reflection coefficient values suggest that the presence of the absorbing material does not impact their operating bandwidth. This was also shown by the simulation results.

As shown in Fig. 7(a), the use of the absorber suppresses transmission levels between 2 to 7 dB in the common operating bandwidth of the antennas for the 1-3-1 tank. The maximum S_{21} values of -56 to -60 dB are observed in the 36.5-37 GHz for both cases, with and without the absorber. We have also calculated the change in transmission caused by the 5% glucose addition for the same frequency range. The differences ΔS_{21} for the five set of measurements were averaged, and the respective error was defined as their standard deviation. As shown in Fig. 8(a), the maximum ΔS_{21} value is 1.5 dB at 36.7 GHz without the absorber, while the value climbs to 3.3 dB when the absorbing material is used.

Figs. 7(a), (b) and 8(a), (b) suggest that the effect of the absorber becomes less significant with the 1-1-1 tank. This is expected as transmission through the sample becomes more dominant when the sample is thinner or less lossy. In the frequency range of interest from 36.5 GHz to 37.5 GHz, the 5% glucose response difference without and with the absorber is 0.75 dB and 0.87 dB, respectively.

V. Conclusion

This paper summarizes our effort to quantify and reduce the impact of diffracted and surface waves on an mm-wave transmission sensing system for glucose monitoring. As direct transmission through the tissue is weak, curved surfaces of tissue cause surface waves to reach the receiving antenna without penetrating the tissue, and these in turn can dominate the received signal. Electric field distributions illustrated this phenomenon and showed that

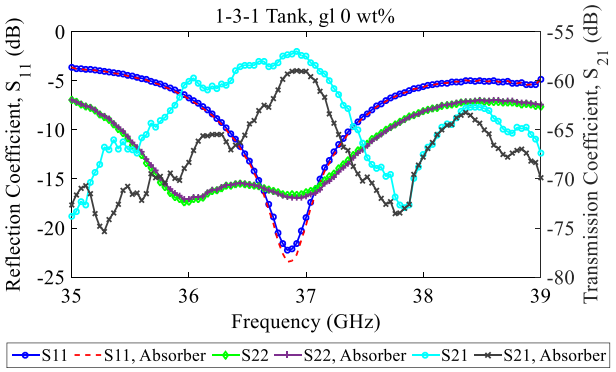

(a)

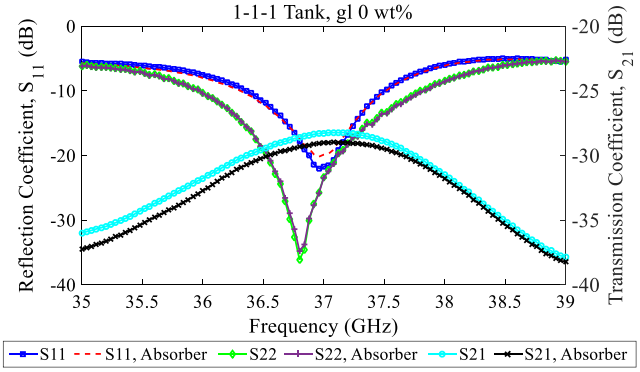

(b)

Figure 7. Transmission S_{21} and reflection coefficients S_{11}, S_{22} with and without the absorber when (a) the 1-3-1 and (b) 1-1-1 tanks are filled with de-ionized water (gl 0 wt%) in the 35-40 GHz range.

signals levels can be almost 40 dB stronger than a reference case simulating locally "infinite" planar surfaces. Moving the antennas further from the tissue's edge to suppress these waves may be impossible for sensor positions such as the earlobe or the area between the thumb and index fingers. Similarly, increasing the power of the source is not a desired solution, especially in case of compact devices.

To test the impact of these unwanted signals on our sensor's sensitivity to glucose changes, we also simulated experiments with acrylic containers filled with solutions of two different glucose concentrations. Simulation results confirmed that suppressing multipath transmission due to diffraction and surface wave propagation can improve signal sensitivity to glucose changes. To suppress these unwanted waves, we used absorbers from commercially available materials, which were placed in a way to block their propagation path.

The acrylic tank simulations allowed us to validate our approach by conducting relevant experiments with our non-invasive glucose sensing prototype. The response of 5 wt% glucose addition in DI water was measured in two acrylic containers of different thickness. Results confirmed that the presence of the absorbers increases the amplitude of the difference in the received signal level with and without the glucose, ΔS_{21}, which translates to an increase in sensitivity to glucose changes [8]. The effect of the absorber was more prominent for the larger tank, but was also beneficial when the thin tank was used. For the larger 1-3-1 tank, the

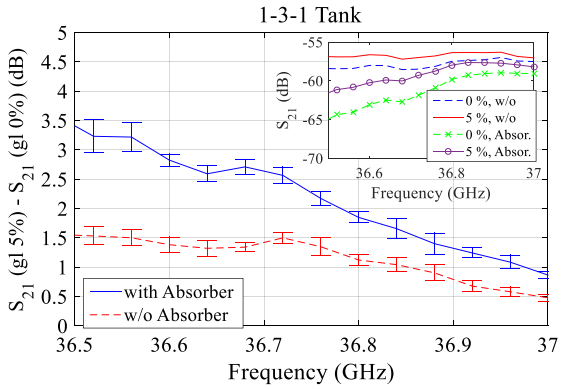

(a)

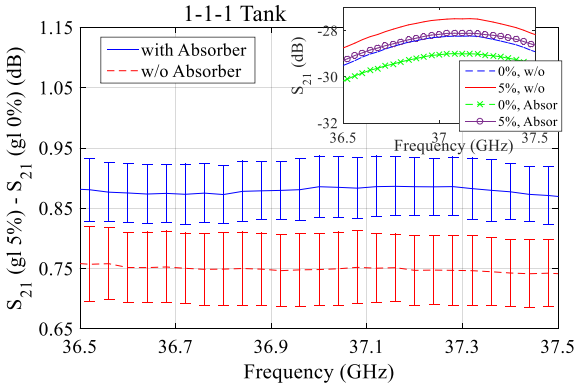

(b)

Figure 8. Difference in the measured transmission coefficient S_{21} due to the addition of 5% glucose in water with (solid line) and without (dashed line) the absorbing material for (a) 1-3-1 and (b) 1-1-1 tanks. Error bars show the standard deviation of the differences (ΔS_{21}) calculated over five measurements. The insets show the actual measured transmission coefficients S_{21} with and without the absorbers for the 1-3-1 and 1-1-1 tanks filled with gl 0 wt% and gl 5 wt% solutions.

increase in ΔS_{21} varied from 70% to 100% in the examined frequency range. For the smaller tank containing a very thin sample, the increase was of the order 15%.

We note that the glucose variations considered in this study are higher than those in diabetes monitoring for better illustrating the effect of surface waves. The sensitivity of our proposed sensor for detecting clinically relevant glucose changes has been studied in detail in [7], [8], where it was shown that the system can detect glucose spikes of 30 mmol/l on porcine and human subjects (transmission changes around 0.7 dB) and 1.3 mmol/l in glucose-loaded water-based samples (changes around 0.01 dB). To enhance the system's sensitivity further, future measurements will be performed with an integrated system comprising the antenna sensors, the absorber, a metamaterial to improve transmission, and auxiliary electronic sensors for calibration. These sensors must capture variations in temperature, motion, and skin hydration due to sweating in order to provide reliable and repeatable measurements [20], [21].Future work will also investigate further the efficiency of the Eccosorb GDS absorbing material. Compact, 3D-printed, metamaterial absorbers have also been recently proposed [22] and will be investigated as a way to increase our sensor's measurement sensitivity to glucose changes.

REFERENCES

[1] H. Cano-Garcia et al., "Detection of glucose variability in saline solutions from transmission and reflection measurements using V-band waveguides," Measurement Science and Technology, vol. 26, no. 12, p. 125701, 2015.

[2] H. Choi et al., "Design and in vitro interference test of microwave noninvasive blood glucose monitoring sensor," system, vol. 19, p. 20, 2015.

[3] J. Vrba, D. Vrba, L. Díaz, and O. Fišer, "Metamaterial Sensor for Microwave Non-invasive Blood Glucose Monitoring," in World Congress on Medical Physics and Biomedical Engineering 2018, 2019, pp. 789–792.

[4] C.-F. So, K.-S. Choi, T. K. Wong, and J. W. Chung, "Recent advances in noninvasive glucose monitoring," Medical Devices (Auckland, NZ), vol. 5, p. 45, 2012.

[5] A. Bauer, O. Hertzberg, A. Küderle, D. Strobel, M. A. Pleitez, and W. Mäntele, "IR-spectroscopy of skin in vivo: Optimal skin sites and properties for non-invasive glucose measurement by photoacoustic and photothermal spectroscopy," Journal of biophotonics, vol. 11, no. 1, p. e201600261, 2018.

[6] R. Pandey et al., "Noninvasive monitoring of blood glucose with raman spectroscopy," Accounts of chemical research, vol. 50, no. 2, pp. 264–272, 2017.

[7] S. Saha et al., "A Glucose Sensing System Based on Transmission Measurements at Millimetre Waves using Micro strip Patch Antennas," Scientific reports, vol. 7, no. 1, p. 6855, 2017.

[8] H. Cano-Garcia, S. Saha, I. Sotiriou, P. Kosmas, I. Gouzouasis, and E. Kallos, "Millimeter-Wave Sensing of Diabetes-Relevant Glucose Concentration Changes in Pigs," Journal of Infrared, Millimeter, and Terahertz Waves, pp. 1–12, 2018.

[9] U. Kaatze, "Complex permittivity of water as a function of frequency and temperature," Journal of Chemical and Engineering Data, vol. 34, no. 4, pp. 371–374, 1989.

[10] G. Conway, W. Scanlon, S. Cotton, and M. J. Bentum, "An analytical path-loss model for on-body radio propagation," in Electromagnetic Theory (EMTS), 2010 URSI International Symposium on, 2010, pp. 332–335.

[11] E. C. Fear, P. M. Meaney, and M. A. Stuchly, "Microwaves for breast cancer detection?," IEEE potentials, vol. 22, no. 1, pp. 12–18, 2003.

[12] F. Topfer and J. Oberhammer, "Millimeter-wave tissue diagnosis: The most promising fields for medical applications," IEEE Microwave Magazine, vol. 16, no. 4, pp. 97–113, 2015.

[13] P. M. Meaney, F. Shubitidze, M. W. Fanning, M. Kmiec, N. R. Epstein, and K. D. Paulsen, "Surface wave multipath signals in near-field microwave imaging," Journal of Biomedical Imaging, vol. 2012, p. 8, 2012.

[14] P. Meaney, S. Pendergrass, M. Fanning, and K. Paulsen, "Importance of using a reduced contrast coupling medium in 2D microwave breast imaging," Journal of Electromagnetic Waves and Applications, vol. 17, no. 2, pp. 333–355, 2003.

[15] S. Ahsan et al., "Design and Experimental Validation of a Multiple-Frequency Microwave Tomography System Employing the DBIM-TwIST Algorithm," Sensors, vol. 18, no. 10, p. 3491, 2018.

[16] P. M. Meaney, C. J. Fox, S. D. Geimer, and K. D. Paulsen, "Electrical Characterization of Glycerin: Water Mixtures: Implications for Use as a Coupling Medium in Microwave Tomography," IEEE transactions on microwave theory and techniques, vol. 65, no. 5, pp. 1471–1478, 2017.

[17] J. Wait, "A note on surface waves and ground waves," IEEE Transactions on Antennas and Propagation, vol. 13, no. 6, pp. 996–997, 1965.

[18] Laird Tecnologies, "Eccosorb® GDS," RFP-DS-GDS 112315.pdf.

[19] D. Andreuccetti, "An Internet resource for the calculation of the dielectric properties of body tissues in the frequency range 10 Hz-100 GHz," http://niremf. ifac. cnr. it/tissprop/, 2012.

[20] S. Rana, R. L. Pricci, P. Kosmas, and E. Kallos, "Motion Artifact Sensor Using Strain Gauges," IEEE Sensors Letters, vol. 3, no. 2, pp. 1–4, 2019.

[21] A. Imam Sunny et al., "Experimental evaluation to detect skin hydration using a bio-impedance sensor," to appear in Proc IEEE EMBC, 2019.

[22] R. Kronberger and P. Soboll, "3D-printed frequency selective surfaces for microwave absorbers," in Antennas and Propagation (ISAP), 2016 International Symposium on, 2016, pp. 178–179.